Radar absorbing and shielding characteristics in ferrite-polymer composites Mn−Zn ferrite/P (TFE-VDF)

© I.M. Isaev, V.G. Kostishin, R.I. Shakirzyanov, A.R. Kayumova, V.K. Olitsky, D.V. Salogub

National University of Science and Technology MISiS,
119049 Moscow, Russia
e-mail: drvgkostishyn@mail.ru

The article discusses the electromagnetic absorbing and shielding properties of ferrite-polymer composites of the composition Mn−Zn ferrite/fluoroplast−42, obtained by pressing a mixture of powders with heating. The measurement of the complex magnetic and dielectric permittivity spectra, as well as the reflection coefficient spectra was carried out in the frequency range 0.1−7 GHz. Using the obtained spectra, a comprehensive analysis of the absorbing characteristics of the composites was carried out, and the factors responsible for the absorption were determined. Fitting of the composites magnetic permeability spectra show that the process of natural ferromagnetic resonance prevails over the resonance of domain walls, and a decrease in the concentration of ferrite inclusions leads to a significant shift in the frequency of natural ferromagnetic resonance to high frequencies. It was found that for composites with a thickness of 5−10 mm, compositions with a mass fraction of ferrite ≤ 0.4 show radio-absorbing properties, while compositions with a fraction of ≥ 0.6 show shielding properties.

Keywords: polymer composite, magnetic properties, radio absorption, feromagnetic resonance, polyvinylidene fluoride, manganese-zinc ferrite.

Introduction

1. Polymer composite materials as electromagnetic radiation absorbers

Radio-absorbing and radio-shielding materials (RAM, RSM) are a special category of materials that enables mitigation of propagation of electromagnetic interferences (EMI) in the space. The relevance of application of RAM has traditionally been related with radio ranging: hiding and stealthiness of weapons and military objects from radio ranging systems due to attenuation or scattering of the reflected signal. In recent years applicability of RAM and RSM has broadly extended to civil applications, such as electromagnetic safety and ecology [1,2], electromagnetic compatibility, noise protection, electromagnetic tests, etc. [3–5].

Assessment of radio-absorbing capability of the materials is usually performed in geometry for reflection. If RAM is located on an ideal reflector (metal), attenuation is provided not only by absorbing EMI inside the material, but also as a result of interferences and compliance with the condition, in which the thickness of material corresponds to the length of the electromagnetic wave (EMW) $\sim \lambda/4$. A measure of absorption in case of the RAM location on metal is the coefficient of reflection (R_l). Dielectric RAM working in the mentioned geometry have narrow absorption range, which is their main fault. More beneficial absorbers of EMI are materials, in which, in addition to interference, EMI is absorbed due to intensive losses during transformation of EMI energy into other types of energy. Thus, magnetic dielectric materials or magnetic polymer composites can be used as combined RAM, which enable expansion of the range of absorption of EMI due to the losses for repolarization, remagnetization, resonance phenomena (natural ferromagnetic resonance (NFMR), domain-wall resonance (DWR)), losses for eddy current and conductivity. Such composites are produced by addition of magnetic, conductive, and dielectric inclusions into polymer matrix. By varying concentration of magnetic filler, the size and the shape of inclusions, one may modify the absorbing capacity within a wide range. Also a big advantage of polymeric composite materials (CM) is their design properties: elasticity, resiliency, easy molding. Efficient RAM in meter and decimeter ranges of EMI are CM based on ferrite-spinel [6–9]. The scientific literature includes a high number of studies of radio-absorbing properties of CM with magnetic fillers of Ni, Co, Zn, Mn, containing ferrite-spinel with such polymer matrices as polyaniline, wax, epoxy resins, polyvinyl alcohol, polyvinylidene fluoride (PVDF) [10–17]. The publications [10,11] studied microwave radio-absorbing properties of composites, where nanoparticles of Co−Zn and particles of Ni−Zn (with replacement of Mg, La) of ferrites were introduced into paraffin matrix. The reflection losses of CM with 80 mass.% fraction of Co−Zn ferrite within the whole X-range were lower than −10 dB (the maximum peak absorption of −23.6 dB at the frequency of 7 GHz) at the CM thicknesses of 3.5−7 mm, meanwhile for CM with the content of 60 mass.% fraction of Ni−Zn ferrite the losses were −10 dB at the frequency

of 15 GHz with the thickness of 3 mm. Composites with conductive additives featuring more losses within the range of 8−12 GHz, e.g., as in the publication [12], where in composites paraffin/Mn−Ni−Zn a polymer with relatively high conductivity (polyaniline) was additionally introduced. In CM with mass fraction of 25% of the composition filler (Mn−Ni−Zn/polyaniline−1/1) the losses were −38.9 dB at the frequency of 9.25 GHz with the thickness of 3.5 mm. PVDF-based CM for radio absorbing were studied in the publications [13–15]. The authors of publication [13] note, that ferrite-polymer composite PVDF/Mn−Cu−Zn-ferrite (nanoparticles filling — 5−25%vol. fraction) has perfect absorbing properties in the range of 8−18 GHz (in the whole range the reflection losses were below −16 dB, with the highest peak value of ~ -32 dB at the frequencies of 11.5 and 14 GHz) and the thickness of 200−300 μm. According to the publication [14], for CM based on Mn−Zn ferrite of the brand 2000NM and PVDF co-polymer (brand F-42), the minimum value R_l at the frequency of 3.2 GHz is −25 dB, and the absorption width Δf is below −10 dB at the frequency of about 2.6 GHz.

In case when the material is on the way of EMW propagation and has no reflectors behind it, the mitigation measure is efficiency of shielding SE_T. Metals feature the best efficiency of shielding. Due to complete reflection of EMI, the intensity of wave behind RSM tends to zero. If it is required to reduce the level of reflected waves, then the magnetic polymer CM can also be efficient. The publication [18] states that for nanocomposite polyaniline/$Ni_{0.6}Cd_{0.4}Fe_2O_4$ with the mass fraction of ferrite of 30% and the thickness of 2.3 mm the shielding efficiency SE_T in the X-range (8−12 GHz) is 41−42 dB, whereas a portion for reflection SE_R is below ~ 8 dB. The study in other publication [19] of absorbing characteristics of nanocomposite with low reflection made of polypyrol/cobalt ferrite/graphene (mass ratio of 1 : 0.5 : 0.3, accordingly) has shown, that $SE_T \sim 37$ dB at $SE_R < 1$ dB.

This study deals with radio-absorbing and radio-shielding properties of composites, where copolymer of polyvinylidene fluoride of the brand F-42 is used as a matrix, and Mn−Zn ferrite-spinel of the brand 2000NM is used as a filler. Analysis of experimental data and mathematical calculations have shown efficiency of the use of obtained composites as RAM and RSM in the range of frequencies of 1−7 GHz.

2. Methods of assessment of absorbing properties of RAM and RSM

As described above, the assessment of absorbing properties of the materials can be performed in two configurations: for reflection (measure — R_l) and for transmission (shielding efficiency, SE_T). The theory of EMW propagation at the RAM−air section boundary is described in electrodynamics through the Maxwell's equations. Another approach during
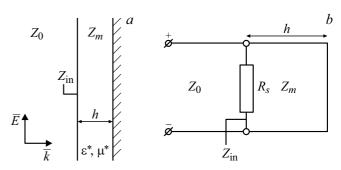

Figure 1. Schematic view of RAM on ideal reflector (*a*) and equivalent electrical diagram (*b*).

modeling of absorbing properties of materials is representation of the RAM−air medium system as the theory of transmission lines, by using such physical magnitudes as relative complex magnetic permittivity μ_r^* and relative complex dielectric permittivity ε_r^*.

If considering the motion of a flat EMW (Fig. 1, *a*), approaching the section boundary, then a part of the wave can be reflected from the boundary. From the Maxwell's equations one may derive condition of the absence of EMW reflection from the boundary of media, which is achieved in case of equality of wave resistances $Z = \sqrt{\mu_0\mu_r^*/\varepsilon_0\varepsilon_r^*}$, i.e. input resistance of RAM Z_{in} and the resistance Z_0. Since RAM work in the air medium, then for one of media one uses the free space wave resistance calculated through the magnetic constant μ_0 and electrical constant ε_0, $Z_0 = \sqrt{\mu_0/\varepsilon_0} = 376.73$ Ω. When calculating R_l, one uses the theory of the transmission line with losses, where the length of the line h corresponds to the sample length. Equivalent electrical diagram for RAM located on an ideal reflector is given in Fig. 1, *b*. The input resistance of short-circuited transmission line with the losses at the distance h can be written as [20]:

$$Z_{in} = Z_m \tanh(-\gamma h), \qquad (1)$$

where $Z_m = Z_0\sqrt{\mu_r^*/\varepsilon_r^*}$ is the wave resistance inside RAM, $\gamma = i\omega c^{-1}\sqrt{\mu_r^*\varepsilon_r^*}$ is the coefficient of propagation.

The coefficient of reflection on the element R_s (resistance of RAM) — $\Gamma = (Z_{in}-Z_0)/(Z_{in} + Z_0)$. The coefficient of reflection in decibels (return losses) is expressed as:

$$R_l = 20 \lg |(Z_{in} - Z_0)/(Z_{in} + Z_0)|. \qquad (2)$$

For EMW transmitted inside the material, the attenuation of electrical and magnetic strengths of the wave (and, therefore, the power) can be assessed by using such term as skin-layer Δ, which reflects the length, at which the EMW amplitude is decreased e times. The less skin-layer, the higher EMI absorption inside the material. The skin-layer is related with the attenuation coefficient $\alpha = 1/\Delta$ (Np/m),

which is written as [21]:

$$\alpha = \frac{\sqrt{2\pi f}}{c}$$

$$\times \sqrt{\mu_r'' \varepsilon_r'' - \mu_r' \varepsilon_r' + \sqrt{(\mu_r'' \varepsilon_r'' - \mu_r' \varepsilon_r')^2 + (\mu_r'' \varepsilon_r' + \mu_r' \varepsilon_r'')^2}}, \tag{3}$$

where μ_r' is the real part of relative complex magnetic permittivity, μ_r'' is the imaginary part of relative complex magnetic permittivity, ε_r' is the real part of relative complex dielectric permittivity, ε_r'' is the imaginary part of relative complex dielectric permittivity.

In turn, the shielding efficiency (in dB) can be determined through the strengths of electrical and magnetic fields as

$$SE_T = 20\lg(E_t/E_0) = 20\lg(H_t/H_0).$$

At $SE_T > 10$ dB the efficiency of shielding consists of two terms of sum — shielding due to reflection SE_R and shielding due to absorption SE_A [18]:

$$SE_T = SE_R + SE_A, \tag{4}$$

which are written as

$$SE_R = 10\lg(1 - R), \tag{5}$$

$$SE_A = 10\lg\big(T/(1 - R)\big), \tag{6}$$

where R is the reflection coefficient in relative units equal to $|S_{11}|^2$, T is the coefficient of transmission in relative units equal to $|S_{12}|^2$.

The efficiency of shielding in magnetic polymer RAM will be assessed by the value SE_A, which indicates a part of EMW power (amplitude) scattered during the losses inside material, whereas $SE_A \gg SE_R$.

3. Experimental part

Experimental samples were obtained by heating of a mixture of polymer and ferrite powders under pressure. Copolymer of polyvinylidene fluoride of the brand F-42 (P(VDF-TFE)) in the powder form was mechanically mixed in porcelain mortar with Mn−Zn ferrite powder of the brand 2000NM. Mixture homogeneity was indirectly evaluated with color change. Ferrite grain size was less

Table 1. Parameters of manufactured samples

№ of sample	C_m,% (ferrite)	C_v (theory), %	h, mm	ρ, g/cm³
1	20	9.0	5.9	2.2
2	40	20.9	6.4	2.5
3	60	37.4	6.3	2.9
4	80	61.4	6.8	3.3

Note. C_m — mass fraction in %, C_v — volume fraction in %, h — thickness of rings, ρ — estimated density of composite.
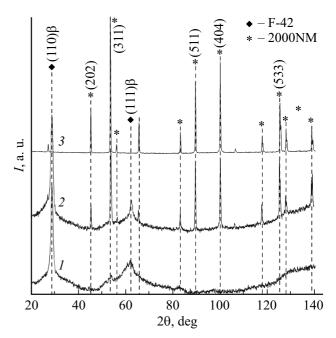

Figure 2. X-ray phase diffractograms of the studied samples: *1* — pure F-42, *2* — composite 20%, *3* — powder 2000NM.

than 45μm. Samples were produced of a ring-shape with outer diameter of 16 mm, inner diameter of 7 mm and the thickness of $h = 5.5-6.8$ mm. Four samples were manufactured during the experiment with the composition according to Table 1. X-ray diffraction analysis of samples and original components was studied in diffractometer „Diffray"401 (radiation CrK_α). Magnetic loops of hysteresis of ferrite powder and composites were obtained by means of vibration magnetometer VM-01M with the maximum magnetic field strength $H = \pm 13$ kOe. For measurement of electromagnetic parameters S_{11}, S_{12}, R_l, ε_r^*, μ_r^* of obtained samples we used vector network analyzer Rohde & Shwartz ZVL-13 with coaxial line designed for the measurement within $0.1-7$ GHz. Summary data on the manufactured experimental samples are given in Table 1.

4. Results and discussion thereof

The results of X-ray analysis of powders of polymer and Mn−Zn ferrite, as well as the composite with 20 mass.% are given in Fig. 2. It is seen that diffractogram of CM includes only reflexes of original components: spinel phase of ferrite powder [22] and reflexes from PVDF (110) and (111) [23]. Similar result is observed also for the rest of CM samples. It can be noted, that in the composite with 20%-content of inclusions the reflex narrowing occurs (111), related with ferroelectric β-phase of PVDF(F-42).

The loops of magnetic hysteresis at the magnetic field strength within ± 3000 Oe of ferrite powder and composites are given in Fig. 3. It is seen that with increase of the mass fraction of ferrite the specific magnetization of CM saturation rises. Table 2 includes magnetic parameters
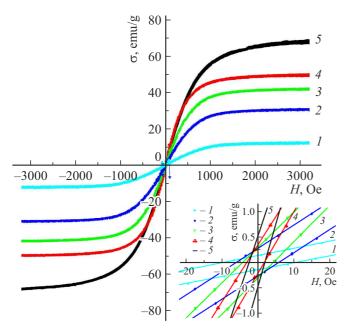
Figure 3. Loops of magnetic hysteresis of the studied samples: *1* — composite 20, *2* — composite 40, *3* — composite 60, *4* — composite 80%, *5* — ferrite powder; insert — view of hysteresis loops in the range $H = 0$ Oe.

Table 2. Static magnetic parameters of the samples under study

Sample	H_c, Oe	σ_r, emu/g	σ_s, emu/g
Powder 2000NM	2.1	0.5	67
CM80%	2.0	0.34	49
CM60%	4.2	0.29	42
CM40%	5.8	0.26	31
CV20%	9.8	0.13	12.4

Note. H_c — coercive force, σ_r — residual magnetization, σ_s — saturation magnetization.

of CM. It can be noted, that saturation magnetization of original powder has a high value 67 emu/g, which is conditioned by the presence of spinel phase only in ferrite. Coercive force of CM rises with the decrease of the mass fraction of inclusions, which, apparently, is caused by the presence of internal degaussing factors (high magnetic polarization).

The dependences of complex dielectric and magnetic permittivity are given in Fig. 4. Appearance of express change of ε_r^* from the frequency in composites with mass fraction of ferrite of 60, 80% in the range of frequencies > 300 MHz is related with excess of the electrical percolation threshold, whose limit for composites with spherical inclusions usually is 15−20 vol.% [24]. This assumption can be explained by a high difference in conductivity of matrix and filler. DC conductivity of PVDF copolymers is ∼ 10^{-12} S/m, meanwhile, depending on Zn content,

Table 3. Parameters of decomposition of magnetic spectra of composites

C_m, %	χ_s	f_r, GHz	χ_d	f_d, GHz	$\beta \cdot 10^{-7}$
20	0.69	2.19	0.34	0.1	3.73
40	1.42	1.58	0.66	0.09	6.36
60	3.45	0.99	1.53	0.1	8.92
80	6.20	0.75	3.08	0.1	7.92

conductivity of Mn−Zn ferrites falls within the range 10^{-9}−10^{-5} S/m [25]. In such case the dispersion view of dependence ε_r^* can be conditioned by the definitive contribution into efficient permittivity of ferrite inclusions. It should also be noted a high significance of ε_r' and ε_r'' of the composite with 80 mass.% of ferrite versus ceramic baked ferrite sample. Similar experimental data were found for epoxy resin/Mn−Zn ferrite ferrite-polymer composites, which are also characterized in a high difference of conductivity of inclusions and matrix [26,27].

The frequency dispersion of complex magnetic permittivity μ_r^* in the studied CM is related with the NFMR and DWR phenomena in ferrite [28]. Often the ranges of NFMR and DWR in the frequency spectrum of ferrite are close that leads to overlapping of spectra of magnetic permittivity from two resonance mechanisms. The specifics of the obtained spectra is dispersion shift, which is expressed as the change of frequency position of the maximum value μ_r'', as well as the frequency of abrupt „bend" μ_r' with the change of inclusions concentration.

In some ferrites, such as Ni−Zn, and polymer composites, where magnetic particles are distributed in non-magnetic medium, the frequency dispersion of complex magnetic permittivity related with NFMR can be with relaxation due to high attenuation of the spin motion. In case of small-size inclusions, the contribution into magnetic permittivity from DWR must be lower, because the number of magnetic domains is reduced. Assessment of DWR and NFMR contributions into magnetic spectra of composites was performed by the formula [28,29]:

$$\mu_r^* = 1 + \frac{f_d^2 \chi_d}{f_d^2 + f^2 + if\beta} + \frac{\chi_s}{1 + j\frac{f}{f_r}}, \qquad (7)$$

where f_d is the DWR frequency, χ_d is the magnetic susceptibility of the domain-walls motion, f_s is the NFMR frequency (relaxation mechanism), χ_s is the magnetic susceptibility of spin motion, β is the coefficient of attenuation of the domain-walls motion, f is the EMI frequency.

Example of decomposition of magnetic permittivity by the formula (7) for composite with 80 mass.% is given in Fig. 5. Summary data of the decomposition of spectra of magnetic permittivity are given in Table 3. Determination of the value of parameters for the equation (7) was performed
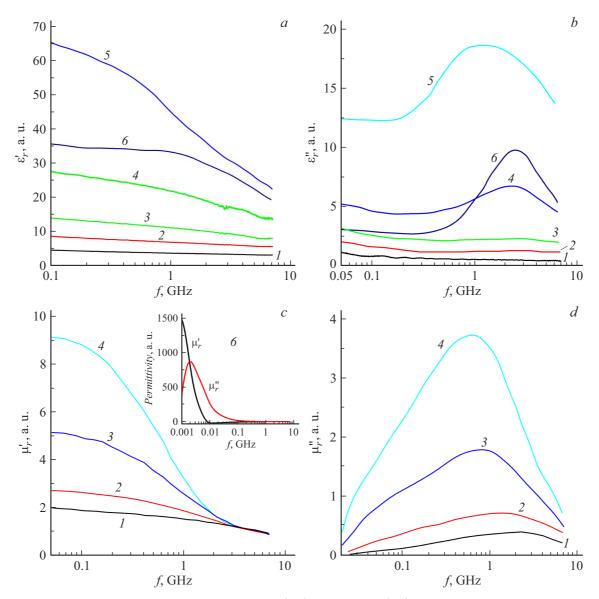
Figure 4. The frequency spectra of relative complex dielectric (a, b) and magnetic (c, d) permittivity for the composites with different mass fraction of ferrite: 1 — F42, 2 — 20, 3 — 40, 4 — 60, 5 — 80%, 6 — 2000NM.

in the software Fityk 1.3.1 by using the least square method (the Levenberg−Marquardt algorithm). Based on the results of decomposition of spectra it can be seen, that the frequency f_r is shifted to the region of high frequencies as far as the mass fraction of ferrite decreases, meanwhile the frequency f_d remains virtually the same regardless of the concentration. Decoposition of magnetic spectrum of pure ferrite 2000N by using the methodology [28] gives the values $\chi_s = 891$, $f_s = 9.69$ MHz, $\alpha = 5.04$, $\chi_d = 871$, $f_d = 6.75$ MHz, $\beta = 1.67 \cdot 10^7$. In baked polycrystalline sample of ferrite the relaxation and resonance frequencies are shifted to the megahertz region, and susceptibility χ_s, χ_d of both mechanisms is very similar.

As indicated in the publication [16], shift of the dispersion region in direction of high frequencies is related with structural inhomogeneity of CM, which is related both with

the structure of inclusions (defect rate), and with their distribution. Availability of non-magnetic interlayer breaks the magnetic flux, and degaussing fields are generated, which change internal efficient magnetic field in CM. Crystal anisotropy, induced anisotropy, and inhomogeneity of the magnetization distribution also have impact to efficient field in polymer magnetic composites. Since the frequency of natural ferromagnetic resonance is directly related with internal efficient field, then the dispersion field shift occurs in CM.

Experimental and calculated spectra R_l, obtained by the formulas (1) and (2), are given in Fig. 6. It can be noted, that frequency position of the maximums of absorption is shifted to the region of low frequencies as far as the sample thickness and mass fraction of ferrite are increased, which correlates with the results of analysis
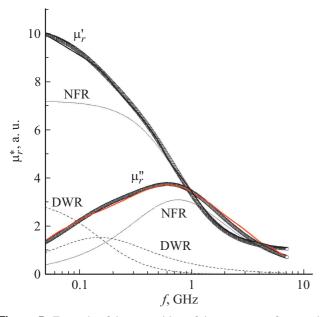
Figure 5. Example of decomposition of the spectrum of magnetic permittivity of composite with mass fraction of ferrite of 80%.

Table 4. Comparison of the absorption parameters of experimental and calculated spectra R_l with a normalized impedance and an interference thickness

C_m, %	h, mm	f_0, GHz	R_l, dB	Δf, GHz	Z_{in}/Z_0	$t_{\lambda/4}$, mm
20	5.9*	5.37	−24.20	2.49	1.10	5.7
20	8	3.64	−20.40	1.83	1.18	7.7
40	6.4*	3.21	−16.80	2.02	0.75	6.4
40	8	2.37	−18.13	1.44	0.80	7.9
60	6.3*	1.41	−10.30	−	0.54	7.0
60	8	1.25	−10.92	0.47	0.62	7.7
80	6.8*	0.55	−10.30	−	0.55	7.2
80	8	0.45	−11.69	0.16	0.62	8.4
40	16.2**	0.98	−49.67	0.52	1.04	15.9
60	20.3**	0.36	−62.22	0.17	1.05	20.1
80	20.2**	0.16	−68.79	0.06	1.04	19.9

Note. * — experimental data, ** — the thickness was calculated by the procedure according to [15].

of magnetic permittivity: the frequency of dispersion μ_r^* for high-concentrated composites also falls within the low-frequency region. Another feature of spectra R_l is that the sample with the 20% ferrite content has the highest losses within the range of thicknesses of CM $5-10$ mm: the minimum value of the coefficient of reflection ~ -20 dB at the width of absorption Δf is less than -10 dB within the range $1-2$ GHz. The maximum absorption in RAM with the geometry to reflection is achieved if two conditions are met: agreement of impedances, at which the normalized impedance $Z_{in}/Z_0 \approx 1$, sample thickness h must be close to the length of the electromagnetic wave (EMW) $\sim \lambda/4$. The thickness $t_{\lambda/4}$ can be determined by the formula:

$$t_{\lambda/4} = nc/(4f_0\sqrt{|\varepsilon_r^* \mu_r^*|}), \qquad (8)$$

where n is the odd natural number $1, 3, 5, \ldots, f_0$ is the frequency of EMI, c is the light speed.

In case of RAM thickness $h = t_{\lambda/4}$, the waves reflected from the sample surface and from the metallic surface are in opposite phase. In order to decrease intensity of the EMI reflected from RAM, the wave amplitudes must be close, which, in turn, depend on permittivity values ε_r^*, μ_r^* [30]. This condition is met at $Z_{in}/Z_0 \approx 1$. Therefore, as we can see from the formulas (1), (8), the maximum absorption depends on combination of the values of permittivity, frequency and thickness of the sample. In order to determine the impact of above mentioned factors to absorption in the studied CM, Table 4 includes comparison of the absorption parameters, $t_{\lambda/4}$, Z_{in}/Z_0 for experimental spectra, as well as for calculated with the thickness of 8 mm. It is seen that the highest values R_l can be viewed for CM with the ratio Z_{in}/Z_0 close to one, and the calculated

value $t_{\lambda/4}$ fails to coincide with the thickness h, except for the sample with $C_m = 40\%$ and $h = 6.4$ mm. Apparently, it could be related with fuzzy absorption peaks; and accurate determination of the frequency of maximum absorption in this case is challenging. The higher the difference between $t_{\lambda/4}$ and h, as well as the deviation Z_{in}/Z_0 from one, the lower absorption. Thus, for the experimental data for the samples with the ferrite content of 60, 80%, the deviation h $t_{\lambda/4} > 0.4$, and $Z_{in}/Z_0 \approx 0.5$, which results in a low value $R_l \sim -10$ dB. Express absorbing properties should be noted for CM with $C_m = 20\%$ and $h = 5.9$ mm: $R_l = -24.2$ dB at 5.37 GHz and the absorption width below -10 dB $\Delta f = 2.49$ GHz, at $Z_{in}/Z_0 = 1.1$. This sample has low density (2.2 g/cm^3), which allows to consider it as perspective RAM with low mass-dimensional characteristics. Calculated values of the parameters of absorption for the fixed thickness $h = 8$ mm show that with increase of concentration of ferrite inclusions, the width of absorption Δf, peak value R_l and its frequency position f_0 are decreased. The [16] describes methodology for finding the thickness h_0 and frequency f_0 for RAM, at which normalized impedance $Z_{in}/Z_0 = 1$. Parameters of absorption of the studied CM for different thicknesses h and concentrations C_m are given in Table 4. It can be seen that increase of concentration of filler elevates peak absorption up to -68.79 dB, but descends the width of absorption Δf down to 0.06 GHz.

Based on the analysis of spectra of tangents of angles of magnetic $\tan \delta_\mu$ and dielectric losses $\tan \delta_\varepsilon$ (Fig. 7), as well as of conductivity, one can see that the losses of EMI are increased with the growth of ferrite concentration in composite. It should be noted, that main losses in
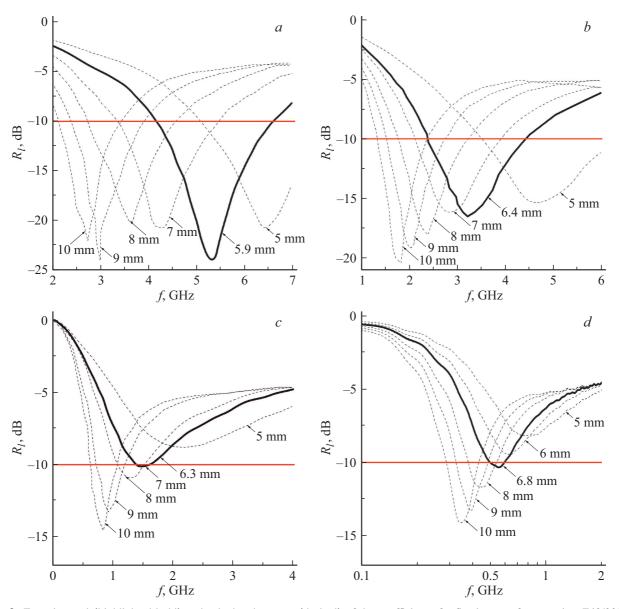
Figure 6. Experimental (highlighted bold) and calculated spectra (dashed) of the coefficient of reflection R_l of composites F42/2000NM with the mass fraction of ferrite 20 (*a*), 40 (*b*), 60 (*c*), 80% (*d*) for thicknesses of $5-10$ mm.

the frequency range $1-7$ GHz are related with magnetic losses, since the values $\tan\delta_\mu$ exceed several times the values $\tan\delta_\varepsilon$. However, for concentrations of 60, 80% the dielectric losses rise significantly versus the samples of 20, 40%. Excess of the electrical percolation threshold increases the intensity of losses due to polarization processes in ferrite and losses for conductivity. High values of tangents of losses, conductivity in composites with the content of 60, 80 mass.% cause low values of skin-layer Δ. The dependences of efficiency of shielding SE_T, SE_R, SE_A of such CM are given in Fig. 8. It is seen that the maximum value SE_T for the composite with $C_m = 80\%$ is ~ -33 dB within the frequency range of $1-7$ GHz, meanwhile SE_R in that range is at least -3 dB. Based on the calculated spectra SE_A, by using the formula $SE_A = -8.686h\alpha$ it

was established that the maximum losses for absorption within the range of $5.5-7$ GHz vary $-18 - -43$ dB with the change of thickness within the limits of $5-10$ mm for CM with 80%, and for CM with 60% — $-10 - -25$ dB. Therefore, high-concentration composites F42/2000N can be considered as efficient RSM with low level of reflected signal for the frequency range of $2-7$ GHz.

Conclusion

This study deals with electromagnetic spectra of ferrite-polymer composites with the composition of F42/2000NM with the mass fraction of ferrite 20, 40, 60, 80%. By using the X-ray fluorescence analysis it was established that during synthesis of composites no formation of new phases
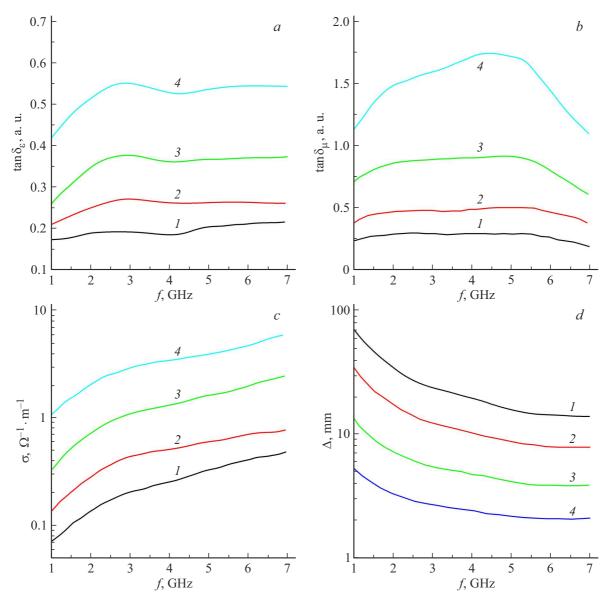
Figure 7. Spectra of tangent of angle of dielectric (*a*) and magnetic (*b*) losses, conductivity (*c*) and skin-layer (*d*) for composites with the mass fraction of ferrite *1* — 20, *2* — 40, *3* — 60, *4* — 80%.

is observed. Magnetic loops of hysteresis of composites indicate the increase of magnetization of samples and decrease of coercive force as far as the ferrite concentration is growing. Spectra of dielectric permittivity, conductivity and tangent of angle of dielectric losses indicate that with the concentrations of 60, 80% there is a rise of dielectric losses in composites. Analysis and decomposition of the spectra of magnetic permittivity show that main contribution into permittivity and losses are caused by the process of gyromagnetic rotation of spin, whereas with the decrease of inclusions concentration the absorption peak position is shifted to the region of high frequencies. Shift of the NFMR frequency results in change of the absorption peak position with the geometry for reflection. Experimental and calculated spectra of the reflection coefficient for composites filled with 20, 40% and thicknesses of 5−10 mm show

that within the frequency range of 2−7 GHz the maximum and minimum peak values R_l are −24 and −15 dB with the width of absorption below −10 dB within the range of 1.5−2.5 GHz. It is explained by compliance with the conditions of agreement of impedances and interference thickness.

In case of high-concentration composites efficient absorption with reflection is possible with the thicknesses exceeding 10 mm. High values of tangents of the angles of losses, therefore, low values of skin-layer cause express shielding properties of composites with the concentration of 60, 80%. Thus, efficiency of shielding SE_T for the frequencies of 1−7 GHz for CM with the mass fraction of inclusions 80% varies within the limits of −15 − −33 dB with the efficiency of shielding due to reflection SE_R of at least −3 dB.
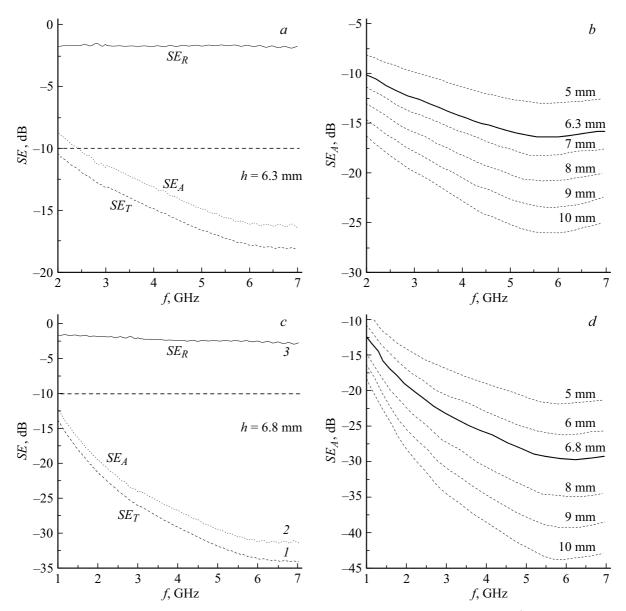
Figure 8. Experimental dependences of efficiency of shielding SE_T, SE_R, SE_A and calculated spectra SE_A (bold line — experimental, dashed — calculated) for the samples with $C_m = 60$ (a, b), 80% (c, d).

Therefore, obtained magnetic polymer composites can be used both as efficient RAM, in which absorbing properties can be modified within a wide range by changing the concentration, and RSM with low level of reflection of electromagnetic radiation.

Funding

Conflict of interest

The authors declare that they have no conflict of interest.

References

[1] Yu.M. Spodobaev, V.P. Kubanov. *Osnovy elektromagnitnoi ekologii* (Radio i svyaz, M., 2000) (in Russian).

[2] P. Thakur, D. Chahar, S. Taneja N. Bhalla, A. Thakur. Ceram. Int., **46**, 15740 (2020). DOI: 10.1016/j.ceramint.2020.03.287

[3] D. Kumar, A. Moharana, A. Kumar. Mater. Today Chem., **17**, 100346 (2020). DOI: 10.1016/j.mtchem.2020.100346

[4] X. Zeng, X. Cheng, R. Yu, G.D. Stucky. Carbon, **168**, 606 (2020). DOI: 10.1016/J.Carbon.2020.07.028

[5] K. Shimada, K. Ishizuka, M. Tokuda. Progr. *In Electromagnetics Research Symposium* (Cambridge, USA, 2006, March 26–29), p. 538.

[6] V.G. Kostishin, R.M. Vergazov, S.B. Men'shova, I.M. Isaev, A.V. Timofeev. Zavodskaya laboratoriya. Diagnostika materialov, **87** (1), 30 (2021) (in Russian).
DOI: 10.26896/1028-6861-2021-87-1-30-34

[7] V.G. Kostishin, R.M. Vergazov, S.B. Men'shova, I.M. Isaev. Ross. tekhnol. zhurn., **8** (6), 87 (2020) (in Russian). DOI: 10.32362/2500-316X-2020-8-6-87-108

[8] I.M. Isaev, V.G. Kostishin, V.V. Korovushkin, D.V. Salogub, R.I. Shakirzyanov, A.V. Timofeev, A.Yu. Mironovich. ZhTF, **91** (9), 1376 (2021) (in Russian). DOI: 10.21883/JTF.2021.09.51217.74-21

[9] M.A. Almessiere, Y. Slimani, A.V. Trukhanov A. Baykal, H. Gungunes, E.L. Trukhanova, S.V. Trukhanov, V.G. Kostishin. J. Ind. Eng. Chem., **90**, 251 (2020). DOI: 10.1016/j.jiec.2020.07.020

[10] A. Poorbafrani, E. Kiani. J. Magn. Magn. Mater., **416**, 10 (2016). DOI: 10.1016/j.jmmm.2016.04.046

[11] Y. Liu, S.C. Wei, Y.J. Wang, H.L. Tian, H. Tong, B.S. Xu. Phys. Procedia, **50**, 43 (2013). DOI: 10.1016/j.phpro.2013.11.009

[12] N.N. Ali, R.A.B. Al-Marjeh, Y. Atassi, A. Salloum, A. Malki, M. Jafarian. J. Magn. Magn. Mater., **453**, 53 (2018). DOI: 10.1016/j.jmmm.2018.01.014

[13] P. Saha, T. Debnath, S. Das, S. Chatterjee, S. Sutradhar. Mater. Sci. Eng. B, **245**, 17 (2019). DOI: 10.1016/j.mseb.2019.05.006

[14] R.I. Shakirzyanov, V.G. Kostishyn, A.T. Morchenko, I. Isaev, V. Kozlov, V. Astakhov. Russ. J. Inorg. Chem., **65** (6), 829 (2020). DOI: 10.1134/S0036023620060194

[15] V.V. Kochervinskii. Bull. Russ. Acad. Sci.: Phys., **84** (2), 144 (2020). DOI 10.3103/S106287382002015X

[16] A.V. Lopatin, N.E. Kazantseva, Yu.N. Kazantsev, O.A. D'yakonova, J. Vilčáková, P. Sáha. J. Comm. Technol. Electron., **53** (5), 487 (2008). DOI: 10.1134/S106422690805001X.

[17] E.V. Yakushko, L.V. Kozhitov, D.G. Muratov, et al. Russ. Phys. J., **63** (12), 2226 (2021). DOI: 10.1007/s11182-021-02292-8

[18] M. Saini, R. Shukla, A. Kumar. J. Magn. Magn. Mater., **491**, 165549 (2019). DOI: 10.1016/j.jmmm.2019.165549

[19] N. Gill, A. L. Sharma, V. Gupta, M. Tomar, O.P. Pandey, D.P. Singh. J. Alloys Compd. **797**, 1190 (2019). DOI: 10.1016/j.jallcom.2019.05.176

[20] D. C. Jenn. *Radar and Laser Cross Section Engineering* (AIAA, 1995), DOI: 10.2514/4.105630

[21] C. Sun, C. Cheng, M. Sun, Z. Zhang. J. Magn. Magn. Mater., **482**, 79 (2019). DOI: 10.1016/j.jmmm.2019.03.034

[22] P. Thakur, D. Chahar, S. Taneja, N. Bhalla, A. Thakur. Ceram. Int., **46** (10), 15740 (2020). DOI: 10.1016/j.ceramint.2020.03.287

[23] V.V. Kochervinskii. Russ. Chem. Rev., **65** (10), 865 (1996). DOI: 10.1070/RC1996v065n10ABEH000328

[24] N.A. Poklonskiy, N.I. Gorbachuk. *Osnovy impedansnoi spektroskopii kompozitov: kurs lektsiy* (BGU, Minsk, 2005) (in Russian).

[25] D. Ravinder, K. Latha. J. Appl. Phys., **75**, 6118 (1994). DOI: 10.1063/1.355479

[26] V.A. Astakhov, R.I. Shakirzyanov, A.T. Morchenko, et al., J. Nano-Electron. Phys., **8** (3), 03044 (2016). DOI: 10.21272/jnep.8(3).03044

[27] A.T. Morchenko. Bull. Russ. Acad. Sci.: Phys., **78** (11), 1209 (2014). DOI: 10.3103/S1062873814110203

[28] T. Tsutaoka. J. Appl. Phys. **93** 2789 (2003) DOI: 10.1063/1.1542651

[29] V. Babayan, N.E. Kazantseva, R. Moučka, I. Sapurina, Yu.M. Spivak, V.A. Moshnikov. J. Magn. Magn. Mater., **324**, 161 (2012). DOI: 10.1016/j.jmmm.2011.08.002

[30] B. Wang, J. Wei, L. Qiao, T. Wang, F. Li. J. Magn. Magn. Mater., **324**, 761 (2012). DOI: 10.1016/j.jmmm.2011.09.011